The Condensing Effect of Cholesterol in Lipid Bilayers

Wei-Chin Hung,* Ming-Tao Lee,† Fang-Yu Chen,‡ and Huey W. Huang§
*Department of Physics, Chinese Military Academy, Fengshan, Kaohsiung, Taiwan; †National Synchrotron Radiation Research Center, Hsinchu, Taiwan; ‡Department of Physics, National Central University, Chung-Li, Taiwan; and §Department of Physics & Astronomy, Rice University, Houston, Texas

ABSTRACT The condensing effect of cholesterol on phospholipid bilayers was systematically investigated for saturated and unsaturated chains, as a function of cholesterol concentration. X-ray lamellar diffraction was used to measure the phosphate-to-phosphate distances, *PtP*, across the bilayers. The measured *PtP* increases nonlinearly with the cholesterol concentration until it reaches a maximum. With further increase of cholesterol concentration, the *PtP* remains at the maximum level until the cholesterol content reaches the solubility limit. The data in all cases can be quantitatively explained with a simple model that cholesterol forms complexes with phospholipids in the bilayers. The phospholipid molecules complexed with cholesterol are lengthened and this lengthening effect extends into the uncomplexed phospholipids surrounding the cholesterol complexes. This long-range thickening effect is similar to the effect of gramicidin on the thickness of lipid bilayers due to hydrophobic matching.

INTRODUCTION

One property that makes cholesterol (and similar sterols) unique among the lipid molecules is its condensing effect on phospholipids in mixtures. This effect was first discovered in monolayer experiments at the air-water interface (1–3) where the area per phospholipid was found to decrease in the presence of cholesterol. The corresponding effect was also found in lipid bilayers. Levine and Wilkins (4) performed the first comprehensive x-ray study on lipid bilayers that included hydrocarbon chain diffraction measuring the orientation distribution of chain segments as well as lamellar diffraction measuring the electron density profiles across the bilayers. Comparing egg lecithin bilayers with mixed bilayers of egg lecithin and cholesterol, they found that cholesterol has the effect of making the hydrocarbon chain segments orient perpendicularly to the plane of the bilayer. Consistent with this effect, cholesterol also increased the phosphate-to-phosphate distance across the bilayer. Subsequently the thickening effect of cholesterol on various phospholipids has been measured by a number of investigators (5–10).

Clearly the condensing effect is more than the molecular interaction between cholesterol and phospholipid. In monolayers, cholesterol causes the area per phospholipid to decrease in a nonideal fashion as a function of cholesterol concentration (1–3). As far as we know this nonideal behavior has not been systematically measured in lipid bilayers. In this article we performed lamellar diffraction to measure the thicknesses of three different mixed bilayers of cholesterol and phospholipids as a function of cholesterol concentration: one phospholipid with two saturated chains, one with two unsaturated chains, and another with one each. We found that all three mixed bilayers increased the thickness with the cholesterol concentration. But the thickness increase is not in proportion to the cholesterol concentration. We will explain this nonlinear condensing effect in terms of a persistence length intrinsic to the elasticity of lipid bilayers, similar to the bilayer thickness modulation due to hydrophobic matching to gramicidin when the latter was incorporated in lipid bilayers (11–13). In many ways, the effect of cholesterol to lipid bilayers is similar to that of gramicidin.

The phase diagrams of liquid-liquid miscibility critical points observed in the monolayer experiments of cholesterol-phospholipid mixtures have been successfully explained by the concept of complex formation (14–19). The interactions of cholesterol and phospholipids at low monolayer pressure are rather complicated because the complexing reaction is reversible. We believe that cholesterol in lipid bilayers, which correspond to monolayers at high surface pressure, is favored to be in the complex form with a negligible rate for decomplexing. This makes it simpler to understand the condensing effect in lipid bilayers.

EXPERIMENTAL METHODS

Materials

1,2-Dimyristoyl-*sn*-glycero-3-phosphocholine (DMPC), 1-stearoyl-2-oleoyl-*sn*-glycero-3-phosphocholine (SOPC), 1,2-dioleoyl-*sn*-glycero-3- phosphocholine (DOPC), and cholesterol (abbreviated as chol in sample compositions) were purchased from Avanti Polar Lipids (Alabaster, AL). Polyethylene glycol (PEG400) was purchased from Merck (Hohenbrunn, Germany). All materials were used as delivered.

Sample preparation

The samples were prepared in the form of oriented multilayers, a stack of parallel lipid bilayers on a solid substrate, the same as used by Levine and

Submitted October 9, 2006, and accepted for publication January 5, 2007.

Address reprint requests to Dr. Huey W. Huang, Dept. of Physics & Astronomy, Rice University, Houston, TX 77251-1892. Tel.: 713-348-4899; Fax: 713-348-4150; E-mail: hwhuang@rice.edu; or Dr. Fang-Yu Chen, Dept. of Physics, National Central University, Chung-Li, Taiwan 32054. Tel.: 886-3-4227151, Ext. 65331; Fax: 886-3-4251175; E-mail: fychen@phy.ncu.edu.tw.

0006-3495/07/06/3960/08 $2.00

doi: 10.1529/biophysj.106.099234

Wilkins (4). The preparation of such oriented samples followed the method described in previous studies (20). Briefly, lipid mixtures were codissolved in a solvent of 1:1 (v/v) methanol and chloroform. The lipid concentration was ~1 mg per 20 μl solvent. The solution of appropriate amount was spread onto a cleaned quartz surface—~100 μl solution onto an 18-mm^2 area. After the solvent evaporated, the sample was placed under vacuum to remove the remaining solvent residues, and then slowly hydrated with water vapor until it appeared transparent.

X-ray lamellar diffraction

The sample for diffraction measurement was kept in a thermally insulated chamber (±0.1°C) that was equipped with mylar windows for x-ray passage. The chamber also enclosed a PEG solution for humidity control (20). The relative humidity corresponding to a PEG solution was measured by a hygrometer (purchased from Rotronic Instrument, Huntington, NY) in a calibration chamber provided by the manufacturer. For example, 1.0 g of PEG400 dissolved in 4.0 g of water gave a vapor pressure equivalent to 98% relative humidity (RH) at 30°C.

The diffractometer consisted of a two-circle goniometer and a Cu K_α radiation source filtered by Ni and operated at 40 kV / 30 mA. The two-circle goniometer was designed for vertical θ–2θ scan, so that the sample substrate was kept nearly horizontal during the entire measurement. This allowed us to measure the lipid samples at full hydration without the problem of sample-running that would otherwise occur if the substrate were oriented vertically as in a horizontal θ–2θ scan experiment. Both the incident and the diffracted x-rays were collimated by two sets of x-y slits. An attenuator was used to prevent the first-order Bragg peak from saturating the detector. Each θ–2θ scan was measured from $\theta = 0.5$–$10.5°$ with a step size $\Delta\theta = 0.01°$ at 1 s per step. The equilibrium of the sample at each humidity setting was ensured by an agreement of at least three consecutive diffraction patterns whose average was subsequently analyzed. Each lipid mixture was measured with at least two separately prepared samples. Each sample was measured twice to check its reproducibility. This procedure also ensured that the samples were not affected by radiation damage. In previous experiments we observed diffraction pattern changes by overexposed samples that also produced extra spots in thin layer chromatography (21).

The procedure for data reduction was described in many of our previous articles (20,22,23). Briefly, the procedure started with the background removal and corrections for absorption and diffraction volume. Then the integrated peak intensities were corrected for the polarization and the Lorentz factors. The magnitude of the diffraction amplitude was the square root of the integrated intensity. The phases were determined by the swelling method (24). With their phases determined, the diffraction amplitudes were Fourier transformed to obtain the transbilayer electron density profiles. The profiles were not normalized to the absolute scale, but they gave the correct phosphate peak-to-phosphate peak distances, since these distances are independent of normalization (22).

RESULTS

In Fig. 1 we display the diffraction patterns measured at 30°C and 98% RH for three series of chol/DMPC, chol/SOPC, and chol/DOPC mixtures. The mol fraction of cholesterol x is defined as $C/(C+L)$, where C and L are the numbers of cholesterol and phospholipid molecules, respectively, in the sample. The condensing effect will be analyzed based on these measurements. When RH exceeded 98% RH, the diffraction patterns of pure PC began to lose high orders and concomitantly the diffraction peaks began to broaden (see, for example, Chen et al. (23)). It is well known that this is due to undulation fluctuations of membranes (25). This phenomenon is common to pure phospholipids. A small osmotic pressure equivalent to 98% RH diminished the undulation fluctuations, thus allowing a more accurate measurement of the electron density profile (23). However, with a cholesterol content exceeding the mol fraction $x \sim 0.1$, the undulation phenomenon disappeared even at full hydration (Fig. 2). It has been known since Levine and Wilkins (4) that the electron density profiles of cholesterol-containing membranes are independent of hydration. Indeed cholesterol has been called a membrane thickness buffer (26). Thus the reason we compare the bilayer thickness at 98% RH, rather than 100% RH, is for the sake of pure PC bilayers. The cholesterol-containing lipid bilayers can be measured at 100% RH without difficulty. The results are the same as measured at 98% RH (see below).

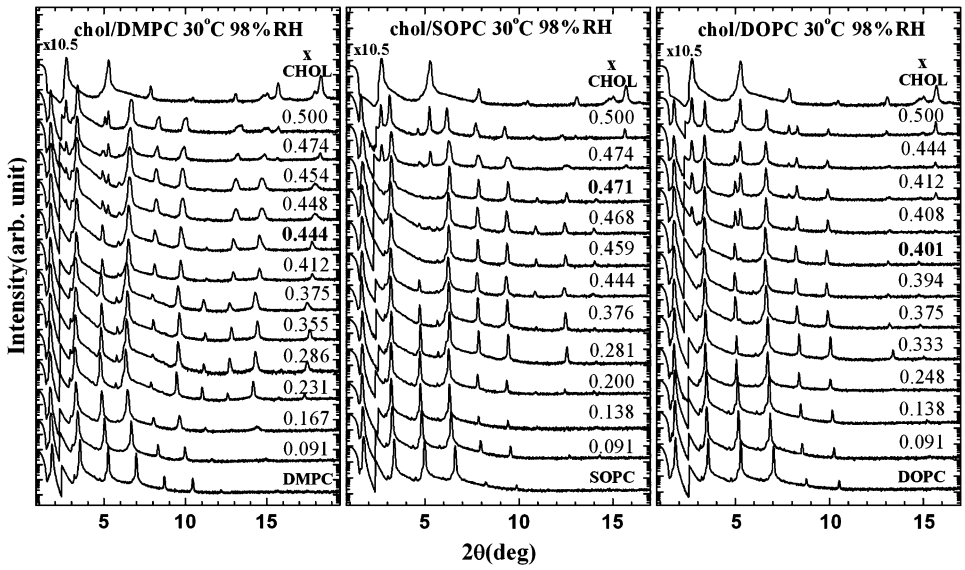

FIGURE 1 Diffraction patterns by multilayers of cholesterol/phospholipid mixtures in series of varying cholesterol mol fraction $x = C/(C+L)$. Separate patterns are displaced vertically for clarity. The top of each panel is the pattern of pure cholesterol. The patterns were measured by θ–2θ scan and an attenuator was used below $2\theta = 2.5°$ (the attenuation factor is 10.5). The patterns above $x = 0.44$ for chol/DMPC, $x = 0.47$ for chol/SOPC, and $x = 0.40$ for chol/DOPC all contain pure cholesterol peaks.

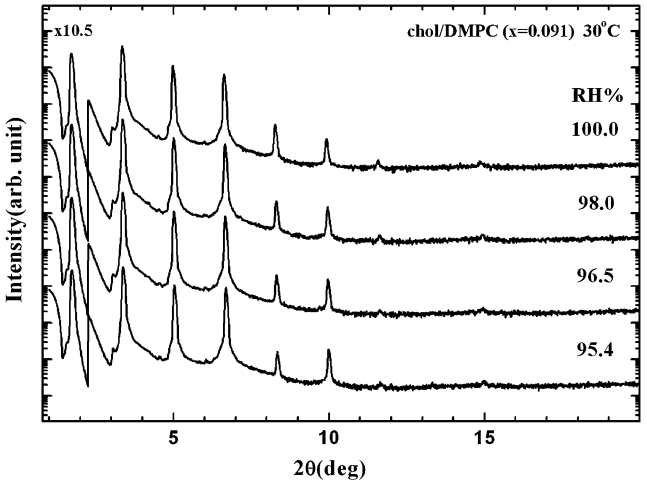

FIGURE 2 Diffraction patterns of cholesterol-containing phospholipid bilayers do not show the membrane undulation effect as the hydration approaches 100% RH, contrary to what would happen to pure phospholipid bilayers (23). (Separate patterns are displaced vertically for clarity.)

Chol/DMPC mixtures

The first column of Fig. 1 shows the diffraction patterns of chol/DMPC mixtures from $x = 0$ (pure PC) to $x = 1$ (pure cholesterol). The pattern on the top is that of pure cholesterol in a crystalline form; cholesterol formed crystals on the substrate as the organic solvent evaporated (see sample preparation).

We know that pure DMPC at 30°C and 98% RH was in the fluid (L_α) phase, exhibiting six diffraction orders. If the hydration level were decreased, DMPC would undergo a phase transition to a gel ($L_{\beta'}$) phase exhibiting nine or more orders (27). To see which phase the chol/DMPC mixtures were in, we measured the diffraction patterns of $x = 0.09$ and $x = 0.17$ over a wide range of RH (Fig. 3). For $x = 0.09$ at 30°C, we see that there is a high-order to low-order transition similar to a gel-fluid transition at 95.1% RH, where two series of lamellar patterns coexisted. At 34°C the transition occurred at 85.1% RH. Such transitions were not detected for $x = 0.17$, where diffraction patterns showed nine or more orders at all humidity levels at 30 and 38°C. Thus we conclude that at 30°C and 98% RH, the chol/DMPC mixture of $x = 0.09$ is in the fluid-like state whereas the chol/DMPC mixtures of $x \geq 0.17$ are in the gel-like state.

From $x = 0.23$ to $x = 0.44$, the diffraction patterns are similar, only the peak intensities systematically vary with x. (A very small peak of unknown origin, at $2\theta \sim 5.7°$, between the third and the fourth peak appeared in all these samples; it will be ignored.) For $x > 0.44$, the patterns include crystalline cholesterol peaks indicating the presence of phase-separated cholesterol domains. Thus in the multilayer preparations, the cholesterol solubility in DMPC bilayers is ~44% in mol fraction. This is comparable to the cholesterol solubility in DMPC measured in aqueous dispersions (28).

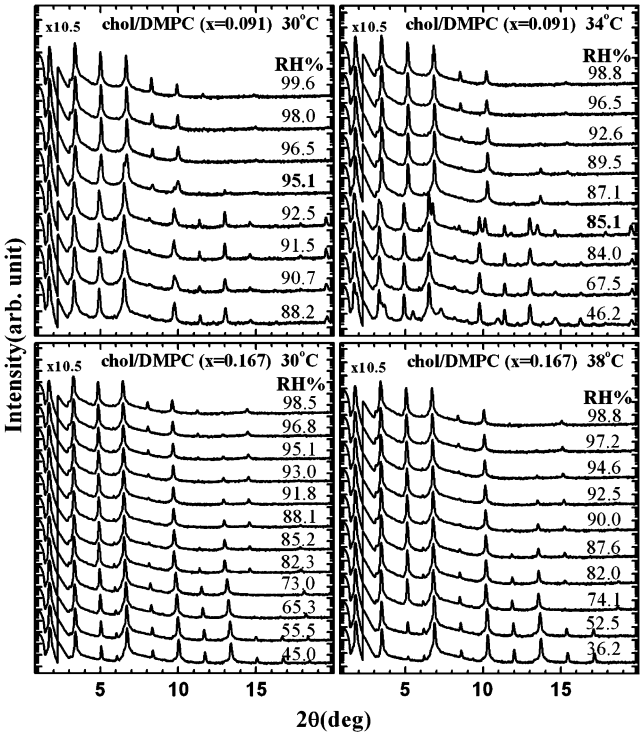

FIGURE 3 Comparison of chol/DMPC at $x = 0.09$ and $x = 0.17$; $x = 0.09$ exhibits two series of lamellar patterns at 95.1% RH, 30°C and at 85.1% RH, 34°C indicating two-phase coexistence, hence a phase transition. No phase transitions were found in the patterns of $x = 0.17$ at 30°C and 38°C. (Separate patterns are displaced vertically for clarity.)

Chol/SOPC mixtures

The diffraction patterns change gradually and systematically from pure SOPC to $x = 0.47$. The patterns for $x > 0.47$ contain cholesterol peaks, indicating the presence of phase-separated cholesterol domains. The solubility of cholesterol in SOPC multilayers is ~47% in mol fraction.

Chol/DOPC mixtures

The diffraction patterns change gradually and systematically from pure DOPC to $x = 0.40$. The patterns for $x > 0.40$ contain cholesterol peaks, indicating the presence of phase-separated cholesterol domains. The solubility of cholesterol in DOPC multilayers is ~40% in mol fraction.

Electron density profiles and phosphate peak-to-phosphate peak distance *PtP*

Each lipid sample shown in Fig. 1 was measured over a range of hydration from ~94% RH to ~98% RH so as to use the swelling method (24) to determine the phases. An example of phasing diagrams is shown in Fig. 4. With the phases determined, the amplitudes from the diffraction patterns were used to construct the transbilayer electron density

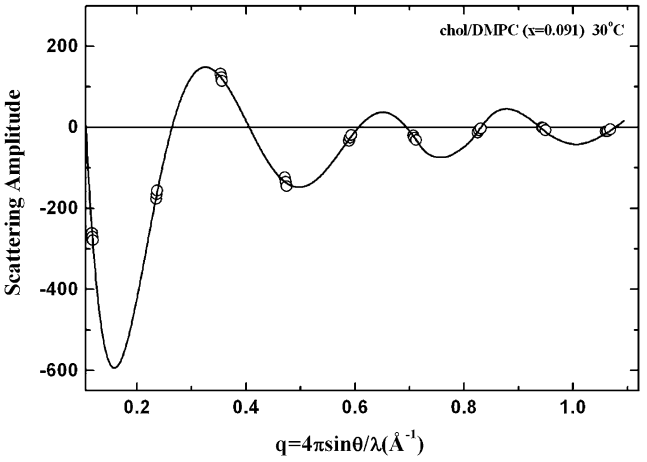

FIGURE 4 An example of phasing diagram. Diffraction by a sample was measured over a range of RH so as to obtain the scattering amplitudes at a series of different lamellar spacings. The scattering amplitudes are either positive or negative. The phases are chosen such that the continuous form factor (*solid curve*) constructed from one set of data at one lamellar spacing goes through all other sets of data (24).

profiles (Fig. 5). The quality of these electron density profiles is comparable to previously published profiles of cholesterol-containing lecithin bilayers that were measured by Franks, Worcester, and Lieb with great care (6,7,26). The distance between the two phosphate peaks across the bilayer (*PtP*) is plotted for each type of mixture as a function of the mol fraction of cholesterol x (Fig. 6). The error bars of *PtP* represent the ranges of values obtained by four to five independent measurements. The errors are generally ± 0.1 Å or smaller.

DISCUSSION

The effect of cholesterol on membrane thickness

As expected from previous measurements (4–10), cholesterol increases the thickness of phospholipid bilayers. Because the chain volume is conserved during chain stretching (this was recently demonstrated experimentally (29)) the thickness increase is directly correlated to the decrease in lipid area, or the condensing effect (Fig. 7). For each type of chol/PC mixture, the *PtP* increases monotonically from that of pure PC to a maximum. The maximum thickness, however, depends on the PC. It is worth noting that the maximum is reached at a mol fraction less than the solubility of cholesterol. The solubilities of cholesterol in DMPC, SOPC, and DOPC multilayers are, respectively, $x(\max) = 0.44$, 0.47, and 0.40 corresponding to $C/L(\max) = 0.80$, 0.89, and 0.68. But in each case, the maximum thickness is reached at $x_o \approx 0.38$, equivalent to $(C/L)_o \approx 0.6$.

The condensing effect and a phenomenological analysis

Between the thickness of pure PC (PtP_{pc}) and the maximum thickness (PtP^*), the increase as a function of the cholesterol content x is not linear. The hypothetical linear increase is shown as a dotted line for each mixture in Fig. 6 *A1*. (Note that the *dotted lines* do not correspond to ideal mixing. An ideal mixing corresponds to the total lipid area being equal to the linear sum of the areas of two components, pure cholesterol and pure PC.) Phenomenologically the data can be fit quite well with the following formula

$$PtP = PtP_{pc}\left(1 - \frac{x}{x_o}\right) + PtP^*\frac{x}{x_o} + \gamma\frac{x}{x_o}\left(1 - \frac{x}{x_o}\right), \quad (1)$$

where x_o is defined as the cholesterol mol fraction when the thickness reaches the maximum. The comparison of the fit with data is shown in Fig. 6 *A1* and, more closely, in Fig. 6 *A2*. The hypothetical linear increases (the *dotted lines* in Fig. 6 *A1*) are described by the first two terms of Eq. 1. Here we assume that the phospholipid molecules directly neighboring a cholesterol molecule are in the maximum thickness PtP^*. In the next section, we will discuss evidence that such thickening effect extends into surrounding cholesterol-free regions over a range determined by the elastic constants of the lipid bilayer. The contribution to the averaged *PtP* by the long-range thickening effect is proportional to the cholesterol content x/x_o and also proportional to the availability of

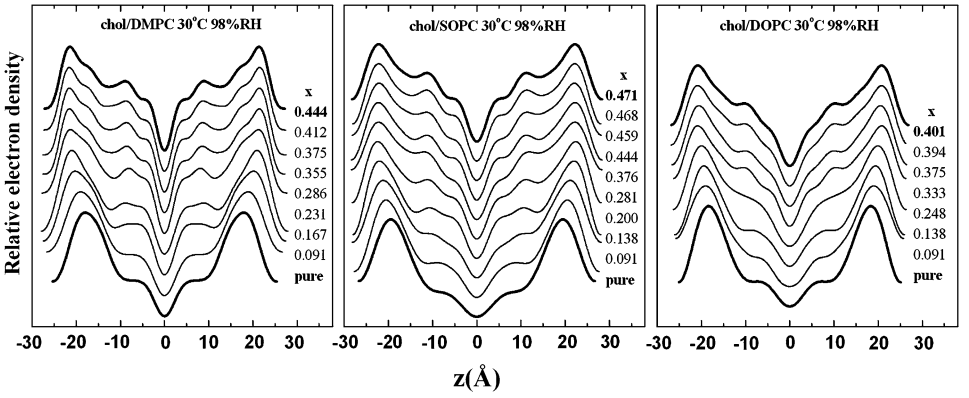

FIGURE 5 Electron density profiles constructed from the diffraction data plotted over one unit cell. Separate profiles are displaced vertically for clarity; z is the coordinate normal to the plane of the bilayer. The origin is chosen at the center of the bilayer. The highest peak on each side is the location of the phosphate group. The phosphate peak-to-phosphate peak distance can be measured very accurately.

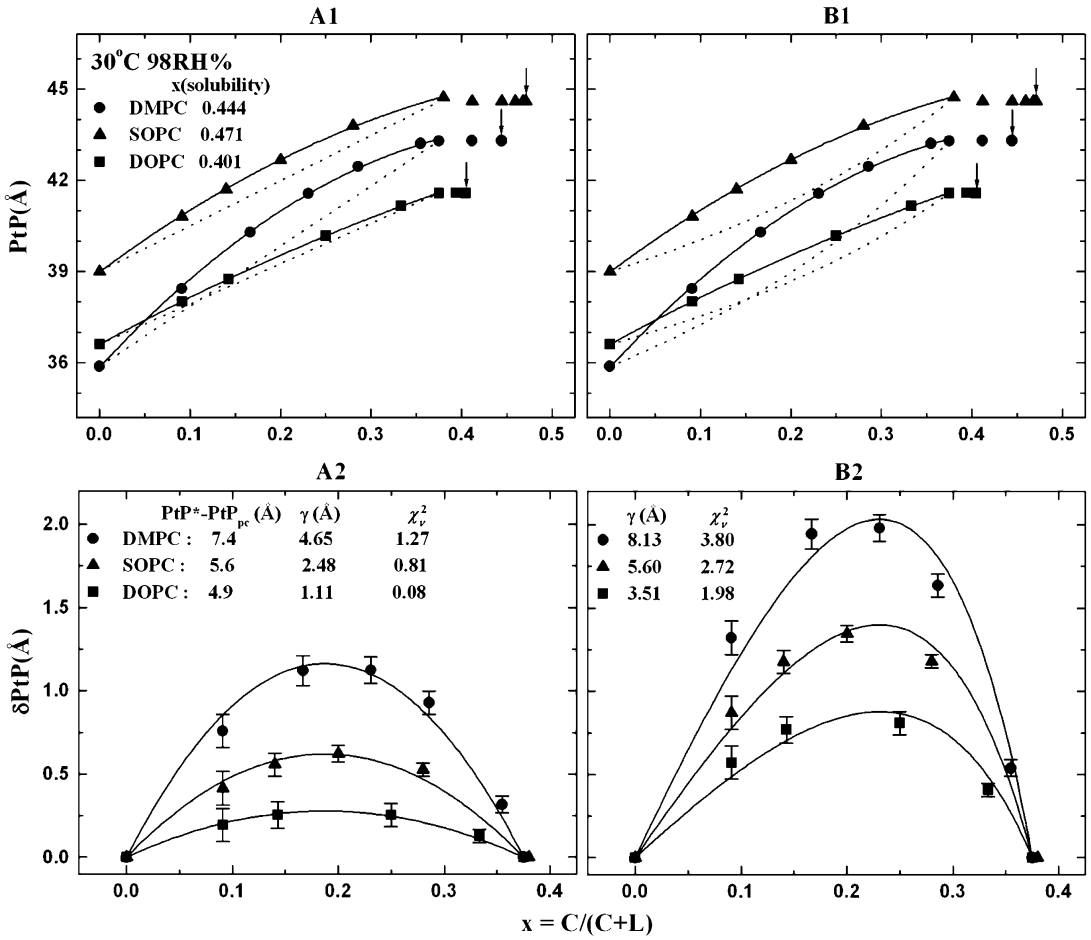

FIGURE 6 *PtP* vs. x and theoretical fit. The error bars in panels *A1* and *B1* are comparable to the size of the symbols used. (*A1*) Equation 1 is used to fit (*solid line*) the data from $x = 0$ to the first data point that reaches the maximum thickness, defined as x_o. The dotted lines are the first two terms of Eq. 1. The arrows indicate the solubility limits. Panel *B1* is the same as *A1* except that Eq. 1 is replaced by Eq. 3. (*A2*) δPtP is the data minus the first two terms of Eq. 1. The solid line is the fit by the third term of Eq. 1. Panel *B2* is the same as *A2* except that Eq. 1 is replaced by Eq. 3. Inset shows the values of $PtP^* - PtP_{pc}$ and the fitting parameter γ, and also $\chi^2_\nu = (N-1)^{-1}\sum_{i=1}^{N}[PtP_i - PtP(eq)_i]^2/\sigma_i^2$ to compare the goodness of fit.

cholesterol-free phospholipids $(1 - x/x_o)$. That explains the third term of Eq. 1 with a constant γ. This phenomenological analysis will now be interpreted in terms of cholesterol complexes.

Cholesterol complex and its long-range effect

The condensing effect gave rise to the idea of cholesterol forming complexes with phospholipids (28,30). In particular the idea explained the observation of pairs of upper miscibility critical points in monolayers of cholesterol-phospholipid mixtures at the air-water interface under low surface pressure (14–19). However, the stoichiometry of the complexes is not definite. It was described as (15,16)

$$qC + pL \leftrightarrow C_qL_p, \tag{2}$$

with unknown values of p and q. In monolayers, Radhakrishnan and McConnell (16) showed that complexing occurs only at temperatures below the gel-fluid transition temperature of the phospholipid. For example, complexing of cholesterol and DMPC was observed in monolayers at 13°C but not in room temperature (the fluid-gel transition temperature of DMPC is ~23°C). Furthermore all complexing phenomena in monolayers were observed at surface pressure below 20 dyn/cm, the pressure considered to be the closest mimic of the corresponding bilayers (16).

The simplest way to understand the condensing effect in lipid bilayers is to assume that in lipid bilayers cholesterol forms complexes with phospholipids practically at all time, namely, the reverse (right to left) reaction in Eq. 2 is negligible. Our experimental results are consistent with cholesterol dispersed uniformly in the bilayer. The simplest model has $q = 1$. We assume that when the cholesterol content reaches x_o, all phospholipid molecules are complexed with cholesterol. Thus the stoichiometric ratio for the complex is $p/q = p = (1 - x_o)/x_o \approx 0.62/0.38 \approx 1.6$. Complexing is not forming a chemical bond. The complexing stoichiometry may fluctuate; p is an average number. The total number

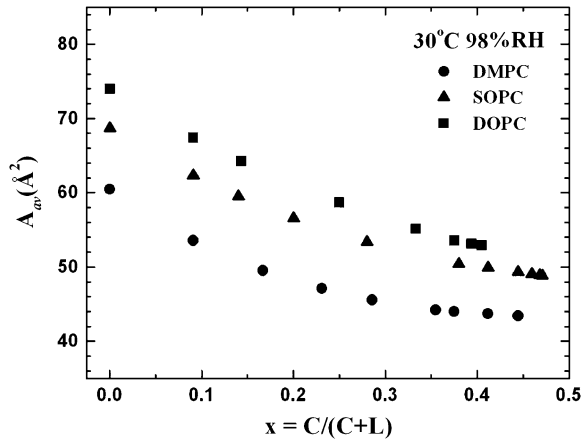

FIGURE 7 Area per molecule as a function of cholesterol concentration. The averaged cross section area of phospholipid is calculated by $A_{av.pc} = 2V_c/(PtP - 10)$, where V_c is the chain volume of the lipid (36), and the thickness of the hydrocarbon region is *PtP* minus twice the length of the glycerol region (from the phosphate to the first methylene of the hydrocarbon chains); the latter is very close to 10 Å (27,33,36). The average area per molecule for the cholesterol-phospholipid mixtures is calculated by $A_{av} = xA_{chol} + (1 - x)A_{av.pc}$. The area per cholesterol A_{chol} is assumed to be constant of x. A value of $A_{chol} \approx 39$ Å^2 was taken from monolayer measurements on pure cholesterol (3,37).

of the complexed lipid molecules, including phospholipid and cholesterol, is $(p+1)C = N(p+1)x = Nx/x_o$, with $N = C + L$. The total number of the cholesterol-free, or uncomplexed phospholipid molecules is $N(1 - x/x_o)$.

The averaged *PtP* is qualitatively explained as follows. Let z be the coordinate normal to the bilayer with the origin at the bilayer center. Let the electron density corresponding to the phosphate peak of the uncomplexed phospholipid molecules be $w_1 \exp[-(z - z_1)^2/\sigma^2]$, where z_1 is the peak position, σ the width of the peak, and w_1 the weight proportional to the total electrons contributing to the peak; and the phosphate peak of the cholesterol complexes be $w_2 \exp[-(z - z_2)^2/\sigma^2]$. Provided $z_2 - z_1$ is substantially smaller then the width σ, the combination of the two peaks will produce a new peak at $\bar{z} \approx (w_1z_1 + w_2z_2)/(w_1 + w_2)$. In Eq. 1, PtP_{pc} and *PtP** correspond to z_1 and z_2, respectively. Equation 1 is obtained if w_1 is proportional to the number of uncomplexed phospholipid molecules $N(1 - x/x_o)$ and w_2 proportional to the number of the complexed lipid molecules, including phospholipid and cholesterol, Nx/x_o. This reproduces the first two terms of Eq. 1. The third term proportional to the product of the two weights $w_1w_2/(w_1 + w_2)^2$ will be discussed below. Although this model reproduces the phenomenological Eq. 1, it assumes that a cholesterol molecule and a phospholipid molecule in the complex contribute equally to the phosphate peak, which is difficult to justify.

In principle, the weight w_2 should include only the complexed phospholipid molecules whose number is $pC = Npx = N(1 - x_o)x/x_o$, while w_1 is proportional to the number of uncomplexed phospholipid molecules $N(1 - x/x_o)$. They should be normalized by the total number of phospholipid molecules $N(1 - x)$. Then according to the formula $\bar{z} \approx (w_1z_1 + w_2z_2)/(w_1 + w_2)$, the Eq. 1 should be modified to

$$PtP = PtP_{pc}\frac{1}{1-x}\left(1 - \frac{x}{x_o}\right) + PtP^*\frac{1 - x_o}{1 - x}\frac{x}{x_o} + \gamma\frac{1 - x_o}{(1 - x)^2}\frac{x}{x_o}\left(1 - \frac{x}{x_o}\right). \quad (3)$$

The fits of Eq. 3 to the data are shown in Fig. 6, *B1* and *B2*.

Both Eqs. 1 and 3 still hold if, for example, $q = 2$, with p changes to $p/2 \approx 1.6$, and so forth. This stoichiometry 2:3.2 for the cholesterol-phospholipid complex determined from the bilayer experiments is very close to the stoichiometry 2:3 determined from monolayer experiments (16).

The modification of the bilayer thickness by cholesterol is similar to the phenomenon of hydrophobic matching to gramicidin channels. A gramicidin channel is a cylindrically shaped dimer with an external hydrophobic surface ~18 Å in diameter and 21.7 Å in height (31,32). A previous experiment found that, when gramicidin was incorporated in lipid bilayers at the peptide/lipid molar ratio 1:10, the *PtP* of DLPC (di12:0PC) increased from 30.8 Å without gramicidin to 32.1 Å with gramicidin, and the *PtP* of DMPC (di14:0PC) decreased from 35.3 Å without gramicidin to 32.7 Å with gramicidin (12). We know that to a very good approximation, the thickness of the hydrocarbon region is $PtP - 10$ Å (27,33,34). Thus the experiment showed that both the hydrocarbon regions of DLPC and DMPC were approaching the hydrophobic thickness of the gramicidin surface ~22 Å. This results show that not only the lipids in contact with gramicidin match their chain lengths to the hydrophobic surface of gramicidin, the effect must extend to the surrounding lipids as well, because the overall thickness of the entire bilayer was approaching the hydrophobic length of gramicidin.

If the hydrocarbon region locally changes its thickness to match the gramicidin's hydrophobic surface, we can use the elasticity theory to calculate the response in the rest of the bilayer (35). The well-established Helfrich energy for membrane deformation (per unit area) can be written as $E_h = (K_a/2)(\delta h/h)^2 + (K_c/8)(\nabla^2 h)^2$ where h is hydrocarbon thickness, and K_a and K_c are, respectively, the stretch and bending moduli. The calculated bilayer deformation due to hydrophobic matching to gramicidin extends to the surrounding lipids over a range $\xi = (16h^2K_c/K_a)^{1/4}$ (35), which is 20–30 Å depending on the values of K_a and K_c. The calculated energy of deformation agreed with the shortening of gramicidin channel lifetime as a function of membrane thickness increase (32,35).

Cholesterol complexing apparently straightens and therefore lengthens the lipid chains (4). This is similar to hydrophobic matching to a surface longer than the normal chain length. Thus we expect that the cholesterol-complexed phospholipids extend the thickening effect, as in the case of hydrophobic matching, to surrounding uncomplexed phospholipid molecules. This effect is stochastic because the distribution of cholesterols is random, as one can see in gramicidin

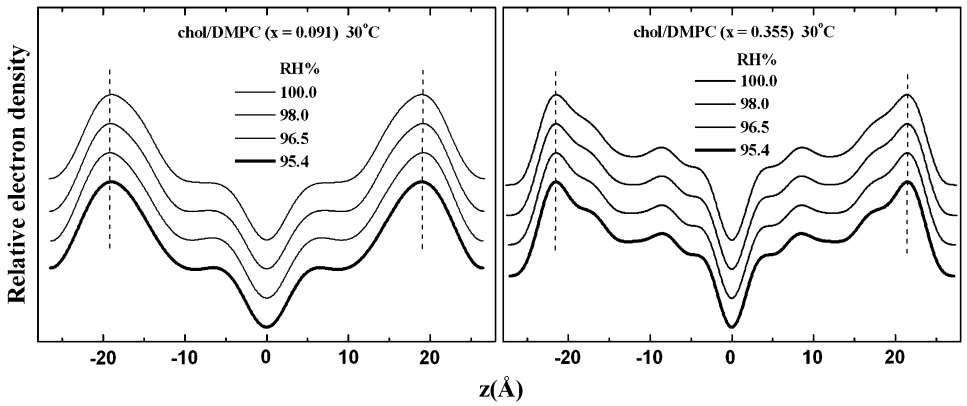

FIGURE 8 Electron density profiles of cholesterol-containing phospholipid bilayers are independent of hydration from ~95% RH to 100% RH, in contrast to pure phospholipids whose profiles vary significantly in this range of RH (23). Separate profiles are displaced vertically for clarity. The dotted lines connecting the peak positions are vertical, indicating no change in the peak positions with hydration.

simulations (Fig. 2 of Harroun et al. (13)); the regions of uncomplexed phospholipid molecules vary in size and shape, and vary with time. The size of some uncomplexed regions may be larger than the persistence length ξ of the thickening effect, but some may be smaller. In average the effect is proportional to the number of the sources, i.e., the complexed lipids, and also proportional to the number of the targets, i.e., the uncomplexed lipids. Hence we have the third terms in Eqs. 1 and 3, respectively.

To view this extended thickening effect, we show δPtP defined as the difference between the data and the first two terms, and compare it with the third term in Fig. 6 *A2* for Eq. 1 and in Fig. 6 *B2* for Eq. 3. Note that given the pure PC and the maximum thicknesses $PtP_{\rm pc}$ and PtP^*, there is no adjustable parameter in the first two terms of either equation. Each curve was fit with only one constant parameter γ in the third term. The fits by Eq. 1 are good but slightly, nevertheless significantly, deviate from the data for DMPC (Fig. 6 *A2*). Upon close inspection, one notices that the data for δPtP are slightly asymmetric with respect to the midpoint between $x = 0$ and $x = x_{\rm o}$, whereas the third term of Eq. 1 is symmetric. In contrast, the fits by Eq. 3 are not as good (the reduced χ-square χ^2_ν is given to compare the goodness of fit in Fig. 6, *A2* and *B2*). However Eq. 3 provides the feature of asymmetry exhibited by the data. Based on the current data alone, it seems as if the correct interpretation for the concentration dependence lies somewhere between Eqs. 1 and 3.

Because the saturated chains can be fully straightened, it is not surprising that DMPC has the largest thickness increase ($PtP^* - PtP_{\rm pc}$). However the thickness increases of SOPC (with one unsaturated chain) and DOPC (with two unsaturated chains) are only ~20% smaller than that of DMPC. What distinguishes the three lipids is the coefficient of the extended thickening effect γ: there is a factor of 1.5–2.0 decrease from DMPC to SOPC and another factor of 1.5–2.0 decrease from SOPC to DOPC.

One more aspect of similarity between the effects of cholesterol and gramicidin needs to be mentioned. Both the cholesterol-containing phospholipid bilayers and the gramicidin-containing phospholipid bilayers showed unvarying electron density profiles over a range of relative humidities ~95–100% (Fig. 8 and Olah et al. (11)). On the contrary, the electron density profiles of pure phospholipid bilayers vary significantly within this range of RH (23). Apparently both cholesterol and gramicidin possess the ability to hold a phospholipid bilayer to a fixed structure. We believe this is possible only by a long-range effect.

According to our definition of cholesterol complexes, after all the phospholipid molecules are complexed to cholesterol, there is still some solubility to additional cholesterol. Thus the maximum solubility, which varies with phospholipid, is higher than the concentration determined by the stoichiometry of the cholesterol complexes.

Mixed monolayers of cholesterol and phospholipids exhibit two upper miscibility critical points at low surface pressure (14,15). These complicated phase diagrams have been successfully explained in terms of a reversible complexing reaction expressed by Eq. 2. This implies that at low cholesterol concentrations (below the complexing stoichiometry) there are two populations of cholesterol, one complexed and another uncomplexed but mixed with phospholipids. Our model implies that, below the solubility limit, all cholesterol molecules in bilayers are complexed with phospholipids. Above the solubility limit, the excessive cholesterol molecules form pure cholesterol domains.

This work was supported by National Science Council (Taiwan) contract Nos. NSC95-2112-M-145-001 (to W.-C.H.), NSC95-2112-M-213-009 (to M.-T.L.), and NSC 94-2112-M-008-021 (to F.-Y.C.), and by National Institutes of Health grant No. GM55203 and the Robert A. Welch Foundation grant No. C-0991 (to H.W.H).

REFERENCES

1. Leathes, J. B. 1925. Condensing effect of cholesterol on monolayers. *Lancet.* 208:853–856.
2. Demel, R. A., L. L. M. Van Deenen, and B. A. Pethica. 1967. Monolayer interactions of phospholipids and cholesterol. *Biochim. Biophys. Acta.* 135:11–19.
3. Phillips, M. C. 1972. The physical state of phospholipids and cholesterol in monolayers, bilayers and membranes. *Prog. Surf. Membrane Sci.* 5:139–222.

4. Levine, Y. K., and M. H. Wilkins. 1971. Structures of oriented lipid bilayers. *Nat. New Biol.* 230:69–72.
5. McIntosh, T. J. 1978. The effect of cholesterol on the structure of phosphatidylcholine bilayers. *Biochim. Biophys. Acta.* 513:43–58.
6. Franks, N. P. 1976. Structural analysis of hydrated egg lecithin and cholesterol bilayers. I. X-ray diffraction. *J. Mol. Biol.* 100:345–358.
7. Worcester, D. L., and N. P. Franks. 1976. Structural analysis of hydrated egg lecithin and cholesterol bilayers. II. Neutron diffraction. *J. Mol. Biol.* 100:359–378.
8. Rappolt, M., M. F. Vidal, M. Kriechbaum, M. Steinhart, H. Amenitsch, S. Bernstorff, and P. Laggner. 2003. Structural, dynamic and mechanical properties of POPC at low cholesterol concentration studied in pressure/temperature space. *Eur. Biophys. J.* 31:575–585.
9. Gallova, J., D. Uhrikova, M. Hanulova, J. Teixeira, and P. Balgavy. 2004. Bilayer thickness in unilamellar extruded 1,2- dimyristoleoyl and 1,2-dierucoyl phosphatidylcholine vesicles: SANS contrast variation study of cholesterol effect. *Colloids Surf. B Biointerfaces.* 38:11–14.
10. Pencer, J., M. P. Nieh, T. A. Harroun, S. Krueger, C. Adams, and J. Katsaras. 2005. Bilayer thickness and thermal response of dimyristoylphosphatidylcholine unilamellar vesicles containing cholesterol, ergosterol and lanosterol: a small-angle neutron scattering study. *Biochim. Biophys. Acta.* 1720:84–91.
11. Olah, G. A., H. W. Huang, W. H. Liu, and Y. L. Wu. 1991. Location of ion-binding sites in the gramicidin channel by X-ray diffraction. *J. Mol. Biol.* 218:847–858.
12. Harroun, T. A., W. T. Heller, T. M. Weiss, L. Yang, and H. W. Huang. 1999. Experimental evidence for hydrophobic matching and membrane-mediated interactions in lipid bilayers containing gramicidin. *Biophys. J.* 76:937–945.
13. Harroun, T. A., W. T. Heller, T. M. Weiss, L. Yang, and H. W. Huang. 1999. Theoretical analysis of hydrophobic matching and membrane-mediated interactions in lipid bilayers containing gramicidin. *Biophys. J.* 76:3176–3185.
14. Radhakrishnan, A., and H. M. McConnell. 1999. Condensed complexes of cholesterol and phospholipids. *Biophys. J.* 77:1507–1517.
15. Radhakrishnan, A., and H. M. McConnell. 1999. Cholesterol-phospholipid complexes in membranes. *J. Am. Chem. Soc.* 121:486–487.
16. Radhakrishnan, A., and H. McConnell. 2002. Thermal dissociation of condensed complexes of cholesterol and phospholipid. *J. Phys. Chem.* 106:4755–4762.
17. Anderson, T. G., and H. M. McConnell. 2002. A thermodynamic model for extended complexes of cholesterol and phospholipid. *Biophys. J.* 83:2039–2052.
18. McConnell, H. M., and A. Radhakrishnan. 2003. Condensed complexes of cholesterol and phospholipids. *Biochim. Biophys. Acta.* 1610:159–173.
19. McConnell, H. 2005. Complexes in ternary cholesterol-phospholipid mixtures. *Biophys. J.* 88:L23–L25.
20. Chen, F. Y., M. T. Lee, and H. W. Huang. 2003. Evidence for membrane thinning effect as the mechanism for peptide-induced pore formation. *Biophys. J.* 84:3751–3758.
21. Wang, W., D. Pan, Y. Song, W. Liu, L. Yang, and H. Huang. 2006. Method of x-ray anomalous diffraction for lipid structures. *Biophys. J.* 91:736–743.
22. Wu, Y., K. He, S. J. Ludtke, and H. W. Huang. 1995. X-ray diffraction study of lipid bilayer membrane interacting with amphiphilic helical peptides: diphytanoyl phosphatidylcholine with alamethicin at low concentrations. *Biophys. J.* 68:2361–2369.
23. Chen, F. Y., W. C. Hung, and H. W. Huang. 1997. Critical swelling of phospholipid bilayers. *Phys. Rev. Lett.* 79:4026–4029.
24. Blaurock, A. E. 1971. Structure of the nerve myelin membrane: proof of the low-resolution profile. *J. Mol. Biol.* 56:35–52.
25. Caille, A. 1972. Physique cristalline:remarques sur la diffusion des rayons X dans les smectiques. *A.C.R. Acad. Sci. Paris Ser. B.* 274: 891–893.
26. Franks, N. P., and W. R. Lieb. 1979. The structure of lipid bilayers and the effects of general anaesthetics. An x-ray and neutron diffraction study. *J. Mol. Biol.* 133:469–500.
27. Hung, W. C., F. Y. Chen, and H. W. Huang. 2000. Order-disorder transition in bilayers of diphytanoyl phosphatidylcholine. *Biochim. Biophys. Acta.* 1467:198–206.
28. Gershfeld, N. L. 1978. Equilibrium studies of lecithin-cholesterol interactions. I. Stoichiometry of lecithin-cholesterol complexes in bulk systems. *Biophys. J.* 22:469–488.
29. Pan, D., W. Wangchen, W. Liu, L. Yang, and H. W. Huang. 2006. Chain packing in the inverted hexagonal phase of phospholipids: a study by x-ray anomalous diffraction on bromine-labeled chains. *J. Am. Chem. Soc.* 128:3800–3807.
30. Subramaniam, S., and H. M. McConnell. 1987. Critical mixing in monolayer mixtures of phospholipid and cholesterol. *J. Phys. Chem.* 91:1715–1718.
31. Arseniev, A. S., I. L. Barsukov, V. F. Bystrov, A. L. Lomize, and YuA. Ovchinnikov. 1985. 1H-NMR study of gramicidin A transmembrane ion channel. Head-to-head right-handed, single-stranded helices. *FEBS Lett.* 186:168–174.
32. Elliott, J. R., D. Needham, J. P. Dilger, and D. A. Hayden. 1983. The effects of bilayer thickness and tension on gramicidin single-channel lifetime. *Biochim. Biophys. Acta.* 735:95–103.
33. McIntosh, T. J., and S. A. Simon. 1986. Area per molecule and distribution of water in fully hydrated dilauroylphosphatidylethanolamine bilayers. *Biochemistry.* 25:4948–4952.
34. Olah, G. A., and H. W. Huang. 1988. Circular dichroism of oriented α-helices. *J. Chem. Phys.* 89:2531–2538.
35. Huang, H. W. 1986. Deformation free energy of bilayer membrane and its effect on gramicidin channel lifetime. *Biophys. J.* 50:1061–1071.
36. Nagle, J. F., and S. Tristram-Nagle. 2000. Structure of lipid bilayers. *Biochim. Biophys. Acta.* 1469:159–195.
37. Scheffer, L., I. Solomonov, M. J. Weygand, K. Kjaer, L. Leiserowitz, and L. Addadi. 2005. Structure of cholesterol/ceramide monolayer mixtures: implications to the molecular organization of lipid rafts. *Biophys. J.* 88:3381–3391.